Original article
DOI: https://doi.org/10.18721/JPM.18103

THE INFLUENCE OF PRESSURE GRADIENTAND LOCAL SURFACE IRREGULARITIES ON THE LAMINAR-TURBULENT TRANSITION IN THE BOUNDARY LAYER

A. V. Garbaruk, V. D. Golubkov✉, *M. Kh. Strelets*

Peter the Great St. Petersburg Polytechnic University, St. Petersburg, Russia

✉ golubkovvd@gmail.com

Abstract. The paper presents the results of a computational study of the effect of longitudinal pressure gradient (PG) on the position of a laminar-turbulent transition (LTT) in the boundary layer both on a smooth plate and a plate with a local surface irregularity. For the former case, the calculations were performed using a procedure (developed recently by the authors) based on the Global Stability Analysis (GSA) of a laminar boundary layer, as well as other well-known methods taking into account the LTT. The results obtained varied significantly for different methods and were different from the more reliable GSA results. This calls into question the accuracy of these methods. The conducted studies have proven the possibility of performing a total assessment of the shift in the LTT by adding the shift occurring due to the change in the PG and the shift for a plate with the surface irregularity in the absence of GD.

Keywords: Tollmien – Schlichting waves, global stability analysis, laminar-turbulent transition, longitudinal pressure gradient

Funding. The reported study was funded by Russian Science Foundation (Grant No. 22-11-00041).

Citation: Garbaruk A. V., Golubkov V. D., Strelets M. Kh., The influence of pressure gradient and local surface irregularities on the laminar-turbulent transition in the boundary layer, St. Petersburg State Polytechnical University Journal. Physics and Mathematics. 18 (1) (2025) 30–41. DOI: https://doi.org/10.18721/JPM.18103

Научная статья
УДК 532.5.013.4
DOI: https://doi.org/10.18721/JPM.18103

ВЛИЯНИЕ ГРАДИЕНТА ДАВЛЕНИЯ И ЛОКАЛЬНЫХ НЕРЕГУЛЯРНОСТЕЙ ПОВЕРХНОСТИ НА ЛАМИНАРНО-ТУРБУЛЕНТНЫЙ ПЕРЕХОД В ПОГРАНИЧНОМ СЛОЕ

А. В. Гарбарук, В. Д. Голубков✉, *М. Х. Стрелец*

Санкт-Петербургский политехнический университет Петра Великого, Санкт-Петербург, Россия

✉ golubkovvd@gmail.com

Аннотация. В статье представлены результаты расчетного исследования влияния продольного градиента давления (ГД) на положение ламинарно-турбулентного перехода (ЛТП) в пограничном слое на гладкой пластине и на пластине с локальной нерегулярностью поверхности. Для гладкой пластины расчеты выполнены с использованием как разработанной авторами методики, основанной на Глобальном Анализе Устойчивости (ГАУ) ламинарного пограничного слоя, так и других известных методов, учитывающих ЛТП. Полученные результаты существенно различаются для разных методов и отличны от более надежных результатов ГАУ, что ставит под сомнение точность этих методов. Проведенные исследования доказали возможность выполнять суммарную оценку сдвига

положения ЛТП путем сложения сдвига для гладкой пластины, имеющего место ввиду изменения величины ГД, и сдвига для пластины с нерегулярностью на ее поверхности в отсутствие ГД.

Ключевые слова: волны Толлмина – Шлихтинга, глобальный анализ устойчивости, ламинарно-турбулентный переход, продольный градиент давления

Финансирование: Работа выполнена при финансовой поддержке Российского научного фонда (грант № 00041-11-22).

Ссылка для цитирования: Гарбарук А. В., Голубков В. Д., Стрелец М. Х. Влияние градиента давления и локальных нерегулярностей поверхности на ламинарно-турбулентный переход в пограничном слое // Научно-технические ведомости СПбГПУ. Физико-математические науки. 2025. Т. 1 № .18. С. 30–41. DOI: https://doi.org/10.18721/JPM.18103

Introduction

Constructing reliable computational methods for finding the position of the laminar-turbulent transition (LTT) is important for many industries (aviation, power and mechanical engineering, etc.), since the aerodynamic forces acting on a streamlined body largely depend on the length of the laminar section of the boundary layer forming on its surface. For example, an increase in the length of the laminar section of the boundary layer in problems of external aerodynamics leads to a decrease in the drag force and, consequently, to a decrease in fuel consumption [1, 2]. LTT is a complex physical process associated with the loss of stability of laminar flow at high (above the critical value) Reynolds numbers. At low levels of turbulence of the external flow, typical for external problems of aerodynamics, Tollmien–Schlichting (TS) waves evolve in the boundary layer, their convective instability inducing well-developed turbulence [3], i.e., the so-called natural LTT scenario unfolds. The evolution of TS waves is influenced by a number of factors; in particular, manufacturing-induced irregularities of the streamlined surface (roughness, small steps and gaps) and the presence of a longitudinal pressure gradient play an important role (see, for example, [4–6]). Accounting for these factors within the framework of parallel and quasi-parallel approximations of classical linear theory of stability [7] does not provide an acceptable accuracy for practical computations of the LTT position. For this reason, in recent years, computational methods based on the so-called global stability analysis (GSA) [8] have become widely popular, which are actively developed and used to solve a wide range of problems in aerodynamics (see, for example, [9–11]).

The methodological problems associated with applying GSA to simulate the evolution of TS waves in a boundary layer, on a flat smooth surface, with a zero pressure gradient have now been largely solved (see [12–14]), and successful applications of GSA to perturbation analysis for 2D or 3D surface inhomogeneities are discussed in [15–17].

A post-processing technique was proposed for the GSA results in [18], allowing to determine the position of the LTT based on the calculated longitudinal distribution of TS wave growth rate in the boundary layer on a smooth plate. This technique was generalized in [19] and applied to calculate the position of the LTT in boundary layers on a plate with local geometric irregularities.

This paper, continuing the research in [18, 19], concentrates on the application of this technique for calculating the position of the LTT under simultaneous influence of irregularities in the surface of the streamlined wall and the pressure gradient.

Technique for determining the LTT position based on GSA

This three-step technique is described in detail in [18–20], so only a brief overview is provided below.

A steady-state solution of 2D unsteady Navier–Stokes equations for compressible ideal gas is found at the first stage:

$$\partial \mathbf{q} / \partial t = \mathbf{RHS}(\mathbf{q}), \tag{1}$$

where $\mathbf{q}$ is the conservative variable vector and $\mathbf{RHS}(\mathbf{q})$ is the right-hand side of the Navier–Stokes equations.

The finite-volume CFD code NTS [21] is used to obtain this solution for $\bar{\mathbf{q}}(x,y)$ whose stability is investigated below using GSA (it is commonly referred to as the baseflow solution). In this case, the spatial approximation of inviscid components of the flux vectors in the right-hand side of expression (1) is carried out using a third-order upwind-biased Roe scheme, and their viscous components are approximated using a second-order central difference scheme. An implicit first-order scheme is used for time integration, and a local (depending on local grid spacings) time step is used to improve convergence to a stationary solution, determined by the given Courant number, in combination with the technique for selective perturbation suppression [22].

At the second stage, GSA of the baseflow solution found at the first stage is performed, where the eigenvalue problem for the Jacobian of the right-hand side of the Navier–Stokes equations (1) $\mathbf{J} = \partial(\mathbf{RHS}) / \partial \mathbf{q} \,|_{\mathbf{q}=\bar{\mathbf{q}}}$ is solved:

$$\mathbf{J}\hat{\mathbf{q}} = \omega \hat{\mathbf{q}}. \tag{2}$$

The solution to this problem, i.e., a set of complex eigenvalues and vectors $(\omega,\hat{\mathbf{q}})$, describes TS waves propagating along the plate. Each pair $(\omega,\hat{\mathbf{q}})$ corresponds to one TS wave (mode). The real part of the eigenvalue ω_r represents the growth or decay rate in the amplitude of this wave over time, its imaginary part ω_i is equal to the frequency of this mode, and the real part of the eigenvector $\hat{\mathbf{q}}(x,y)$ represents the spatial distribution of the wave amplitude.

Problem (2) is solved numerically for a discrete analogue of the Jacobian for which the calculation method was provided in our paper [23]. In this case, the Krylov–Schur method is used, implemented in the SPEPc/PETSc open library [24].

Finally, at the third and final stage, the post-processing of GSA results (pairs of eigenvalues and eigenvectors) is carried out, which makes it possible to determine the position of the LTT. This post-processing technique, described in detail in [19] consists of calculating the growth rate of individual TS waves $N_\omega(x)$ and constructing their envelope $N(x)$. After that, the LTT position is determined as the coordinate x_t at which $N(x_t)$ reaches the critical value N_{crit}.

In this paper, it is assumed that this value depends only on freestream turbulence level and is determined by the Mack formula [25]:

$$N_{crit} = -8.43 - 2.4 \cdot \ln(Tu).$$

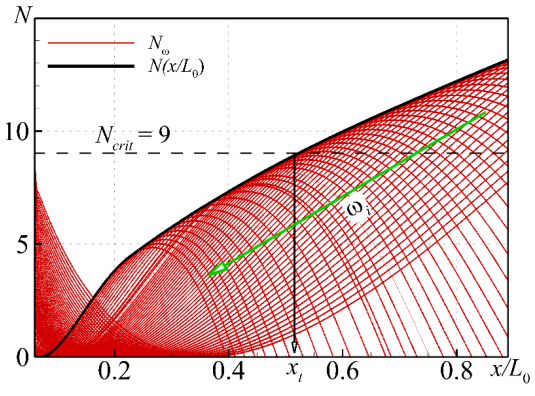

Fig. 1 Construction of envelope for Tollmien–Schlichting wave growth rate $N(x)$ in the boundary layer on flat plate and determination of transition position x_t at $N_{crit} = 9$
The green arrow indicates the direction of frequency growth

Fig. 1 shows an example of determining the LTT position x_t in the boundary layer on a smooth flat plate at a value $N_{crit} = 9$, corresponding to freestream turbulence level $Tu = 0.07\%$.

Problem statements

A boundary layer on a flat surface is considered in the presence of a longitudinal pressure gradient generated by tilting the upper boundary of the computational domain (Fig. 2) on which a free-slip condition is imposed.

The computational domain for the first stage of the calculations (obtaining the baseflow solution) includes the plate with the L_0 and a section of the 'slippery' wall in front of it ($-0.1 \le x/L_0 < 0.0$), which is necessary for correct description of the formation of a laminar boundary layer in the inlet section of the plate [19].

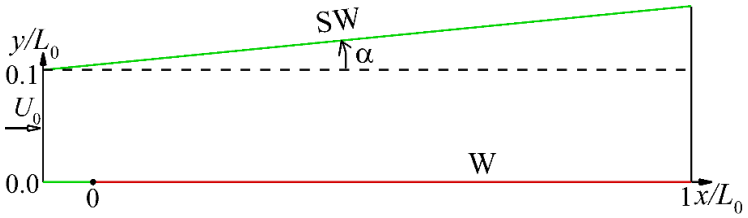

Fig. 2. Schematic of computational domain. Problem: calculate the baseflow solution for a boundary layer on a plane plate (length L_0) with a pressure gradient;
W, SW are the wall and the slip wall, respectively; α is the slope of the upper boundary of the computational domain; U_0 is the inlet velocity of compressible ideal gas

The characteristic Reynolds (Re_0) and Mach (M) numbers, based on the inlet velocity U_0 and the plate length L_0, are equal to

$$Re_0 = U_0 L_0/\nu = 6\cdot 10^6;$$

$$M = 0.05,$$

where ν is the dynamic viscosity of the gas.

The height of the inlet section of the channel is fixed ($y/L_0 = 0.1$), while the height ratio of its outlet and inlet sections varies from 0.975 to 1.050 with a step of 0.025, corresponding to a change in the inclination angle α of the upper boundary of the computational domain from about −0.13 to +0.26°; according to calculations, this provides an almost constant value of the dimensionless pressure gradient σ:

$$\sigma = \frac{\nu}{\rho U_0^3}\frac{dp}{dx},$$

where ρ is the gas density; dp/dx is the dimensional pressure gradient.

The magnitude of σ varies in the range from $-4.8\cdot 10^{-9}$ to $6.1\cdot 10^{-9}$. Specific computations were performed for four values of σ, equal to

$$-4.8\cdot 10^{-9};\ 0.0;\ 2.8\cdot 10^{-9};\ 6.1\cdot 10^{-9},$$

i.e., with a favorable (negative), zero, and two unfavorable (positive) pressure gradients.

In addition to the smooth bottom plate, simulations were performed in the presence of a backward-facing step located at $x/L_0 = 0.25$ with a variable height.

$$h/\delta^*_0 = 0.25;\ 0.50;\ 0.75,$$

where $\delta^*_0 = 3.5\cdot 10^{-4} L_0$ is the local displacement in the boundary layer without a pressure gradient at $x/L_0 = 0.25$.

The boundary conditions for calculating the baseflow solution were imposed as follows.

Homogeneous velocity and temperature profiles were set at the inlet boundary, and the remaining variables were extrapolated to it from within the computational domain.

The free slip condition was imposed on the upper (inclined) boundary and on the lower one at $-0.1 \le x/L_0 < 0.0$, while the no-slip and no-flow conditions were imposed on the rest of the lower boundary ($x/L_0 \ge 0$) for velocity, and an adiabatic condition was imposed for temperature.

Finally, a constant pressure was set at the outlet boundary, and the remaining variables were extrapolated to it from inside the computational domain.

The dimensions of the computational domain and the boundary conditions remained unchanged in the presence of a backward-facing step, except that the lower boundary shifted downwards by h at $x/L_0 \ge 0.25$, forming a step.

The spacings of the computational grids were set approximately equal to the spacings of the grids used in [19], where they were confirmed to provide a grid-independent baseflow solution. As a result, the grid sizes ranged from 2.4 million cells (for a smooth plate) to 3.7 million cells (for a plate with a step).

The computational domain for GSA is part of the computational domain used to obtain the baseflow solution. In particular, its inlet boundary shifts downstream to $x/L_0 = 0.05$, the outlet boundary is located at $x/L_0 = 0.90$, and the upper boundary at $y/L_0 = 0.06$. In addition, homogeneous Dirichlet conditions were used at all boundaries as boundary conditions for perturbations. The rationale for this choice of the size of the computational domain and the boundary conditions for GSA is given in [19].

Comparison of GSA results with results of other methods for computation of LTT in the presence of longitudinal pressure gradient

This section presents a comparison of LTT positions in the boundary layer on a smooth flat surface at different values of longitudinal pressure gradients calculated by GSA with the results obtained by other methods (a locally parallel approximation of classical linear stability theory [7] and the Drela method [26], based on correlations constructed using solutions of the Falkner–Skan equation). In addition, the GSA results were compared with similar results of the two most popular semi-empirical turbulence models for RANS equations that take into account LTT, namely, the differential γ-Re_θ SST model [27] and the algebraic alg-γ SST model [28]. The boundary conditions at the inlet boundary of the computational domain for the transport equations of turbulent characteristics in these models were imposed based on the ratio of turbulent and molecular viscosities $\nu_t/\nu = 1$ and the turbulence level $Tu = 0.07\%$, which, as already mentioned, corresponds to the critical value of the N-factor $N_{crit} = 9$.

The results of the comparison are shown in Figs. 3 and 4.

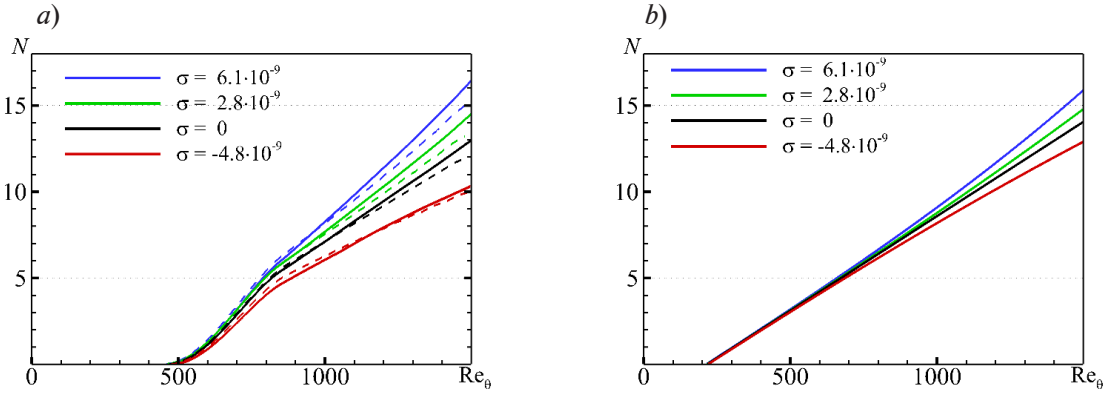

Fig. 3. Calculated effect of pressure gradient on longitudinal distribution of growth rate $N(Re_\theta)$ of TS waves on flat plate: GSA and locally parallel approximation were used (a, solid and dashed curves, respectively) ; calculations by the Drela method (b)

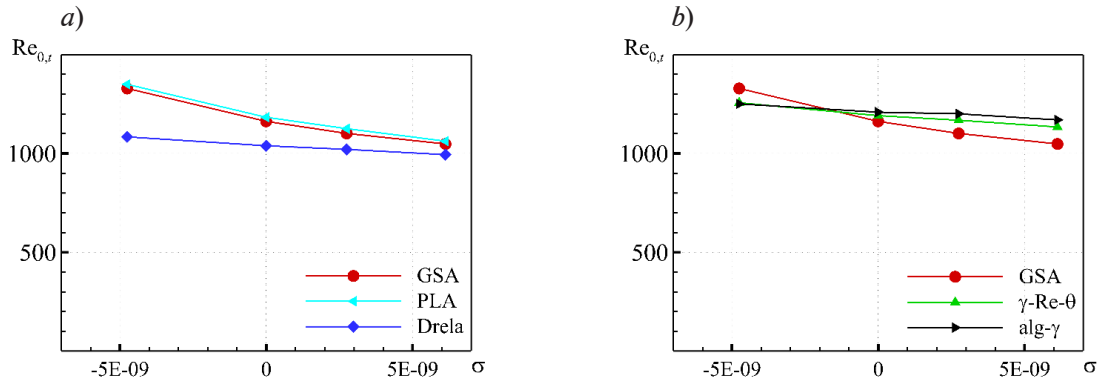

Fig. 4. Dependences of LTT position $Re_{\theta,t}$ on dimensionless pressure gradient σ (obtained from GSA results) compared with similar dependences obtained by locally parallel approximation (PLA) and Drela method (a), as well as LTT models for RANS equations (b)

In particular, Fig. 3 compares the dependences of TS wave growth rate on the Reynolds number Re_θ constructed from the local momentum thickness, which are calculated using three of the considered methods based on stability analysis. Evidently, all three methods accurately characterize the well-known trend towards stabilization of the boundary layer (towards a decrease in the growth rate N) with a decrease in the pressure gradient. However, the Drela method predicts a

noticeably slower increase in the value of $N(\mathrm{Re}_\theta)$ with a decrease in the pressure gradient compared with GSA and the locally parallel approximation, which is likely because the Drela method uses correlations based on the Falkner–Skan solution.

Fig. 4 shows the dependences of the LTT Reynolds number $\mathrm{Re}_{\theta,t}$ on the dimensionless pressure gradient, determined by the corresponding curves $N(\mathrm{Re}_\theta)$ obtained using different methods with a critical value of the N-factor equal to 9. Fig. 4,*a*, which compares the results of GSA, the locally parallel approach, and the Drela method, fully reflects the trends discussed above in the analysis of Fig. 3: the results of the first two methods are close to each other, while the Drela method predicts an earlier LTT for all pressure gradients considered and a weaker sensitivity to them. As for the LTT models for RANS equations (γ-Re_θ SST and alg-γ SST), they predict similar values of LTT $\mathrm{Re}_{\theta,t}$ for all pressure gradients considered (see Fig. 4,*b*). These values practically coincide with the results obtained by GSA in the boundary layer with a weak pressure gradient (the value of σ is close to zero), considerably differing from GSA results when σ deviates from zero. In other words, GSA predicts a much stronger influence of the pressure gradient on the position of the LTT than the LTT models for RANS equations. We also note that the latter results are close to the results obtained by the Drela method in this respect.

Analysis of combined effect of pressure gradient and surface irregularity in the form of backward-facing step on LTT position

The combined effect of these factors on the longitudinal distribution of TS wave growth rate is illustrated in Fig. 5. Evidently, this indicator increases monotonically with increasing pressure gradient at any step height, increasing sharply in the vicinity of the step. The dependence $N(\mathrm{Re}_\theta)$ becomes close to linear again further downstream, the same as in the absence of the step.

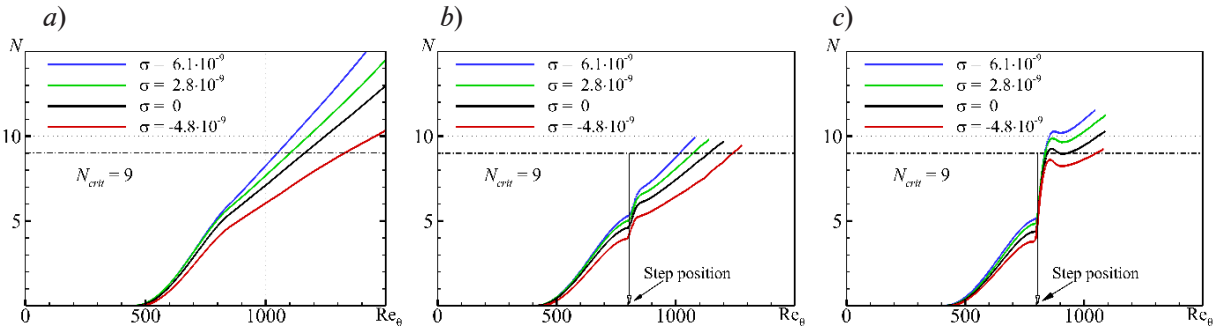

Fig. 5. Dependences of TS wave growth rate on local Reynolds number Re_θ at different pressure gradients for boundary layer on flat plate without step (*a*) and with steps of height $h/\delta^*_0 = 0.25$ (*b*) and 0.75 (c)

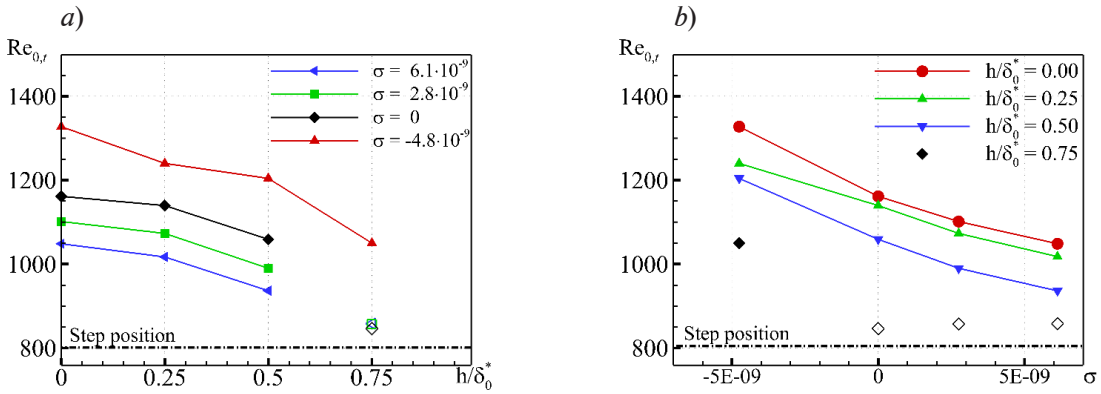

Fig. 6. Dependence of LTT position on pressure gradient at different step heights (*a*) and on step height at different pressure gradients (*b*)

Fig. 6 shows the dependences of the number $\mathrm{Re}_{\theta,t}$ corresponding to LTT position on the magnitude of the pressure gradient σ at fixed values of h/δ_0^* and on the height of the step h/δ_0^* at fixed values of σ. These results were obtained from the data shown in Fig. 5 with a critical growth rate equal to 9. Analyzing the dependences in Fig. 6, we can conclude that two LTT scenarios can be implemented on the surface with steps: natural (associated with the development of TS instability) and bypass [4], which occurs in the immediate vicinity of the step (empty symbols in Fig. 6).

The second scenario is observed for the step with a height of $h/\delta_0^* = 0.75$ with non-negative pressure gradients. For all cases of natural LTT (shaded symbols in Fig. 6), $\mathrm{Re}_{\theta,t}(\sigma)$ curves at different fixed step heights (see Fig. 6,*a*) and $\mathrm{Re}_{\theta,t}(h/\delta_0^*)$ curves at fixed pressure gradients (see Fig. 6,*b*) are qualitatively similar to each other. This suggests that the influence of the pressure gradient and the step height on the position of the natural LTT turns out to be independent (additive), i.e., it can be approximately described by the following relation:

$$\Delta \mathrm{Re}_{\theta,t}\left(\sigma, h/\delta_0^*\right) = \Delta \mathrm{Re}_{\theta,t}\left(\sigma, 0\right) + \Delta \mathrm{Re}_{\theta,t}\left(0, h/\delta_0^*\right), \tag{3}$$

where $\Delta \mathrm{Re}_{\theta,t}\left(\sigma, h/\delta_0^*\right) = \mathrm{Re}_{\theta,t}\left(\sigma,\ h/\delta_0^*\right) - \mathrm{Re}_{\theta,t}\left(0,0\right)$ is the total variation in the LTT $\mathrm{Re}_{\theta,t}$ due to the influence of both the pressure gradient σ and the height of the step h/δ_0^*, while $\Delta\mathrm{Re}_{\theta,t}(\sigma,0)$ and $\Delta\mathrm{Re}_{\theta,t}(0,h/\delta_0^*)$ are its variations due to only the influence of the pressure gradient at zero step height and only the step height at zero pressure gradient, respectively.

The table shows the relative errors of calculations by Eq. (3), found by the formula

$$\Delta, \% = \left[\Delta \mathrm{Re}_{\theta,t}\left(\sigma, h/\delta_0^*\right) - \Delta \mathrm{Re}_{\theta,t}\left(\sigma, 0\right) - \Delta \mathrm{Re}_{\theta,t}\left(0, h/\delta_0^*\right)\right] \Big/ \mathrm{Re}_{\theta,t}\left(0,0\right) \cdot 100\%. \tag{4}$$

Table

Relative error of calculations by Eq. (3) as function of dimensionless pressure gradient σ and step height h/δ_0^*

σ, 10^{-9}	Relative error Δ, %		
	$h/\delta_0^* = 0.25$	$h/\delta_0^* = 0.50$	$h/\delta_0^* = 0.75$
–4.8	–5.6	–1.8	3.3
2.8	–0.5	–0.8	Bypass
6.1	–0.8	–0.8	LTT

Note. The values of Δ were found by Eq. (4).

It follows from the data in Table that the error is less than 1% for positive (unfavorable) pressure gradients, and 3.3% for a negative gradient, which generally confirms the hypothesis of an additive effect of the pressure gradient and the height of the step on the position of the natural LTT in the considered range of parameters.

Conclusion

The paper reports on the results of computational studies performed using the global stability analysis (GSA) technique and aimed at assessing the effect of a longitudinal pressure gradient and the presence of a local irregularity in the form of a backward-facing step on the position of a natural (resulting from Tollmien–Schlichting instability) laminar-turbulent transition in a boundary layer on a flat surface. This study further develops the technique we constructed in our earlier works.

The computational results for boundary layers on smooth surfaces in the presence of a pressure gradient are compared with similar results obtained using approximate methods of classical stability theory and the most accurate of the available closure models for RANS equations, accounting for the transition.

This comparison showed that the GSA results differ dramatically from those obtained by the Drela method [26], based on correlations constructed by stability analysis of the Falkner–Skan family of profiles, and from the results obtained by models accounting for the transition within

RANS equations (γ-Re_θ SST[27] and alg-γ SST [28] models). This conclusion is very important, as it calls into question the accuracy of these methods, which are currently widely used in practical computations.

The results of a parametric study on the simultaneous effect of a pressure gradient and the presence of a step on the surface on the transition indicate that the effect of these two factors on the position of the laminar-turbulent transition can be approximately considered independent (additive) in the given range.

The simulations were run on the Polytechnic RSC Tornado cluster of the Polytechnic Supercomputer Center (http://www.spbstu.ru).

REFERENCES

1. **Crouch J. D.,** Boundary-layer transition prediction for laminar flow control (Invited report), Proc. 45th AIAA Fluid Dynamics Conf. 22–26 June, 2015, Dallas, TX, AIAA 2015-2472, 2015.

2. **Malik M. R, Crouch J. D., Saric W., et al.,** Application of drag reduction techniques to transport aircraft (Chapter), In book: R. Blockley, W. Shyy (Eds.), Encyclopedia of Aerospace Engineering, John Wiley & Sons, Ltd., Hoboken, New Jersey, USA, December (2015) 1–10.

3. **Boiko A. V., Dovgal A. V., Grek G. R., Kozlov V. V.,** Physics of transitional shear flows: Instability and laminar–turbulent transition in incompressible near-wall shear layers (Book Series "Fluid Mechanics and Its Applications", Vol. 98), Springer Science & Business Media B.V., Dordrecht, Netherlands, 2011.

4. **Crouch J. D., Kosorygin V. S., Sutanto M. J., Miller G. D.,** Characterizing surface-gap effects on boundary-layer transition dominated by Tollmien – Schlichting instability, Flow. 2 (22 March) (2022) E8.

5. **Heintz A., Scholz P.,** Measurements on the effect of steps on the transition of laminar boundary layers, Exp. Fluids. 64 (4) (2023) 76.

6. **Teng M., Piomelli U.,** Instability and transition of a boundary layer over a backward-facing step, Fluids. 7 (1) (2022) 35.

7. **Reed H. L., Saric W. S., Arnal D.,** Linear stability theory applied to boundary layers, Annu. Rev. Fluid Mech. 1996. Vol. 28 (1) (1996) 389–428.

8. **Theofilis V.,** Global linear instability, Annu. Rev. Fluid Mech. 43 (Jan) (2011) 319–352.

9. **Swaminathan G.,** Global stability analysis of non-parallel flows: PhD Thesis, Jawaharlal Nehru Centre for Advanced Scientific Research, Bangalore, India, 2010.

10. **Bucci M. A., Puckert D. K., Andriano C., et al.,** Roughness-induced transition by quasi-resonance of a varicose global mode, J. Fluid Mech. 836 (10 Febr) (2018) 167–191.

11. **Timme S.,** Global instability of wing shock-buffet onset, J. Fluid Mech. 885 (25 Febr) (2020) A37.

12. **Ehrenstein U., Gallaire F.,** On two-dimensional temporal modes in spatially evolving open flows: the flat-plate boundary layer, J. Fluid Mech. 536 (10 Aug) (2005) 209–218.

13. **Ekervik E., Ehrenstein U., Gallaire F., Henningson D. S.,** Global two-dimensional stability measures of the flat plate boundary-layer flow, Eur. J. Mech. B. Fluids. 27 (5) (2008) 501–513.

14. **Alizard F., Robinet J.-C.,** Spatially convective global modes in a boundary layer, Phys. Fluids. 19 (11) (2007) 114105.

15. **Garicano-Mena J., Ferrer E., Sanvido S., Valero E.,** A stability analysis of the compressible boundary layer flow over indented surfaces, Comput. Fluids. 160 (4 Jan) (2018) 14–25.

16. **Mathias M., Medeiros M. F.,** Global instability analysis of a boundary layer flow over a small cavity, Proc. AIAA Aviation 2019 Forum, 17–21 June, 2019. AIAA 2019-3535, American Institute of Aeronautics and Astronautics, Dallas, Texas, USA, 15 June, 2019.

17. **Kuester M. S.,** Growth of Tollmien – Schlichting waves over three-dimensional roughness, Proc. AIAA Scitech 2020 Forum, 6–10 Jan., 2020, AIAA 2020-1580, American Institute of Aeronautics and Astronautics, Dallas, Texas, USA, 5 January, 2020.

18. **Belyayev K., Garbaruk A., Golubkov V., Strelets M.,** Computation of evolution of Tollmein – Schlichten waves based on the global stability analysis, Math. Models Comput. Simul. 16 (1) (2024) 29–38.

19. **Belyaev K., Garbaruk A., Golubkov V., Strelets M.,** Prediction of effect of small local surface irregularities on natural transition to turbulence based on Global Stability Analysis, Int. J. Heat Fluid Flow. 107 (July) (2024) 109358.

20. **Belyaev K. V., Garbaruk A. V., Golubkov V. D., Strelets M. Kh.,** Application of global stability analysis to predicting characteristics of Tollmien – Schlichting waves, St. Petersburg Polytechnic University Journal. Physics and Mathematics. 16 (1.1) (2023) 218–224.

21. **Shur M., Strelets M., Travin A.,** High-order implicit multi-block Navier – Stokes code: Ten-2025 experience of application to RANS/DES/LES/DNS of turbulence, Proc. 7th Symp. Overset Composite Grids and Solution Technology. Oct. 5–7, 2004, Huntington Beach, CA, USA (2004) 5–7.

22. **Richez F., Leguille M., Marquet O.,** Selective frequency damping method for steady RANS solutions of turbulent separated flows around an airfoil at stall, Comput. Fluids. 132 (25 June) (2016) 51–61.

23. **Garbaruk A., Golubkov V.** A comparison of two approaches to the global stability analysis using the example of the cylinder flow problem, St. Petersburg Polytechnic University Journal. Physics and Mathematics. 16 (4) (2023) 50–62 (in Russian).

24. **Hernandez V., Roman J.E., Vidal V.,** SLEPc: A scalable and flexible toolkit for the solution of eigenvalue problems, ACM Trans. Math. 31 (3) (2005) 351–362.

25. **Mack L. M.,** Transition and laminar instability. 15 May, 1977. https://api. semanticscholar.org/ CorpusID:118505937.

26. **Drela M., Giles M. B.,** Viscous-inviscid analysis of transonic and low Reynolds number airfoils, AIAA J. 25 (10) (1987) 1347–1355.

27. **Langtry R. B., Menter F. R.,** Correlation-based transition modeling for unstructured parallelized computational fluid dynamics codes, AIAA J. 47 (12) (2009) 2894–2906.

28. **Menter F. R., Matyushenko A., Lechner R., et al.,** An algebraic LCTM model for laminar–turbulent transition prediction, Flow, Turbul. Combust. 109 (4) (2022) 841–869.

СПИСОК ЛИТЕРАТУРЫ

1. **Crouch J. D.** Boundary-layer transition prediction for laminar flow control (Invited report) // Proceedings of the 45th AIAA Fluid Dynamics Conference. 22–26 June, 2015. Dallas, TX, American Institute of Aeronautics and Astronautics, AIAA 2015-2472, 2015.

2. **Malik M. R, Crouch J. D., Saric W., Lin J. C, Whalen E. A.** Application of drag reduction techniques to transport aircraft (Chapter) // R. Blockley, W. Shyy (Eds.) Encyclopedia of Aerospace Engineering. Hoboken, New Jersey, USA: John Wiley & Sons, Ltd., 2015. December. Pp. 1–10.

3. **Boiko A. V., Dovgal A. V., Grek G. R., Kozlov V. V.** Physics of transitional shear flows: Instability and laminar–turbulent transition in incompressible near-wall shear layers (Book Series "Fluid Mechanics and Its Applications", Vol. 98). Dordrecht, Netherlands: Springer Science+Business Media B.V., 2011. 272 p.

4. **Crouch J. D., Kosorygin V. S., Sutanto M. J., Miller G. D.** Characterizing surface-gap effects on boundary-layer transition dominated by Tollmien – Schlichting instability // Flow. 2022. Vol. 2. 22 March. P. E8.

5. **Heintz A., Scholz P.,** Measurements on the effect of steps on the transition of laminar boundary layers // Experiments in Fluids. 2023. Vol. 64. No. 4. P. 76.

6. **Teng M., Piomelli U.** Instability and transition of a boundary layer over a backward-facing step // Fluids. 2022. Vol. 7. No. 1. P. 35.

7. **Reed H. L., Saric W. S., Arnal D.** Linear stability theory applied to boundary layers // Annual Review of Fluid Mechanics. 1996. Vol. 28. No. 1. Pp. 389–428.

8. **Theofilis V.** Global linear instability // Annual Review of Fluid Mechanics 2011. Vol. 43. January. Pp. 319–352.

9. **Swaminathan G.** Global stability analysis of non-parallel flows: PhD Thesis. Bangalore, India: Jawaharlal Nehru Centre for Advanced Scientific Research, 2010. 152 p.

10. **Bucci M. A., Puckert D. K., Andriano C., Loiseau J.-Ch., Cherubini S., Robinet J.-Ch., Rist U.** Roughness-induced transition by quasi-resonance of a varicose global mode // Journal of Fluid Mechanics. 2018. Vol. 836. 10 February. Pp. 167–191.

11. **Timme S.** Global instability of wing shock-buffet onset // Journal of Fluid Mechanics. 2020. Vol. 885. 25 February. P. A37.

12. **Ehrenstein U., Gallaire F.** On two-dimensional temporal modes in spatially evolving open flows: the flat-plate boundary layer // Journal of Fluid Mechanics. 2005. Vol. 536. 10 August. Pp. 209–218.

13. **Ekervik E., Ehrenstein U., Gallaire F., Henningson D. S.** Global two-dimensional stability measures of the flat plate boundary-layer flow // European Journal of Mechanics-B/Fluids. 2008. Vol. 27. No. 5. Pp. 501–513.

14. **Alizard F., Robinet J.-C.** Spatially convective global modes in a boundary layer // Physics of Fluids. 2007. Vol. 19. No. 11. P. 114105.

15. **Garicano-Mena J., Ferrer E., Sanvido S., Valero E.** A stability analysis of the compressible boundary layer flow over indented surfaces // Computers & Fluids. 2018. Vol. 160. 4 January. Pp. 14–25.

16. **Mathias M., Medeiros M. F.** Global instability analysis of a boundary layer flow over a small cavity // AIAA Aviation 2019 Forum. 17–21 June, 2019. Dallas, Texas, USA: American Institute of Aeronautics and Astronautics, AIAA 2019-3535,15 June, 2019.

17. **Kuester M. S.** Growth of Tollmien – Schlichting waves over three-dimensional roughness // AIAA Scitech 2020 Forum. 6–10 January, 2020. Orlando, FL, USA: American Institute of Aeronautics and Astronautics, AIAA 2020-1580, 5 January, 2020.

18. **Беляев К. В., Гарбарук А. В., Голубков В. Д., Стрелец М. Х.** Расчет эволюции волн Толлмина – Шлихтинга на основе глобального анализа устойчивости // Математическое моделирование. 2023. Т. 35. № 9. С. 45–60.

19. **Belyaev K., Garbaruk A., Golubkov V., Strelets M.** Prediction of effect of small local surface irregularities on natural transition to turbulence based on Global Stability Analysis // International Journal of Heat and Fluid Flow. 2024. Vol. 107. July. P. 109358.

20. **Belyaev K. V., Garbaruk A. V., Golubkov V. D., Strelets M. Kh.** Application of global stability analysis to predicting characteristics of Tollmien – Schlichting waves // St. Petersburg Polytechnic University Journal. Physics and Mathematics. 2023. Vol. 16. No. 1.1. Pp. 218–224.

21. **Shur M., Strelets M., Travin A.** High-order implicit multi-block Navier – Stokes code: Ten-2025 experience of application to RANS/DES/LES/DNS of turbulence // Proceedings of the 7th Symposium on Overset Composite Grids and Solution Technology. October 5–7, 2004, Huntington Beach, CA, USA. 2004. Pp. 5–7.

22. **Richez F., Leguille M., Marquet O.** Selective frequency damping method for steady RANS solutions of turbulent separated flows around an airfoil at stall // Computers & Fluids. 2016. Vol. 132. 25 June. Pp. 51–61.

23. **Голубков В. Д., Гарбарук А. В.** Сравнение двух подходов к глобальному анализу гидродинамической устойчивости на примере задачи обтекания цилиндра // Научно-технические ведомости СПбГПУ. Физико-математические науки. 2023. Т. 16. № 4. С. 50–62.

24. **Hernandez V., Roman J.E., Vidal V.** SLEPc: A scalable and flexible toolkit for the solution of eigenvalue problems // ACM Transactions on Mathematical Software. 2005. Vol. 31. No. 3. Pp. 351–362.

25. **Mack L. M.** Transition and laminar instability. 15 May, 1977. https://api.semanticscholar.org/CorpusID:118505937.

26. **Drela M., Giles M. B.** Viscous-inviscid analysis of transonic and low Reynolds number airfoils // AIAA Journal (American Institute of Aeronautics and Astronautics). 1987. Vol. 25. No. 10. Pp. 1347–1355.

27. **Langtry R. B., Menter F. R.** Correlation-based transition modeling for unstructured parallelized computational fluid dynamics codes // AIAA Journal. 2009. Vol. 47. No. 12. Pp. 2894–2906.

28. **Menter F. R., Matyushenko A., Lechner R., Stabnikov A., Garbaruk A.** An algebraic LCTM model for laminar–turbulent transition prediction // Flow, Turbulence and Combustion. 2022. Vol. 109. No. 4. Pp. 841–869.

THE AUTHORS

GARBARUK Andrey V.
Peter the Great St. Petersburg Polytechnic University
29 Politechnicheskaya St., St. Petersburg, 195251, Russia
agarbaruk@mail.ru
ORCID: 0000-0002-2775-9864

GOLUBKOV Valentin D.
Peter the Great St. Petersburg Polytechnic University
29 Politechnicheskaya St., St. Petersburg, 195251, Russia
golubkovvd@gmail.com
ORCID: 0000-0001-9473-7430

STRELETS Michael Kh.
Peter the Great St. Petersburg Polytechnic University
29 Politechnicheskaya St., St. Petersburg, 195251, Russia
strelets@mail.rcom.ru
ORCID: 0000-0002-4608-388X

СВЕДЕНИЯ ОБ АВТОРАХ

ГАРБАРУК Андрей Викторович – *доктор физико-математических наук, доцент Высшей школы прикладной математики и вычислительной физики Санкт-Петербургского политехнического университета Петра Великого.*
195251, Россия, г. Санкт-Петербург, Политехническая ул., 29
agarbaruk@mail.ru
ORCID: 0000-0002-2775-9864

ГОЛУБКОВ Валентин Денисович – *младший научный сотрудник Высшей школы прикладной математики и вычислительной физики Санкт-Петербургского политехнического университета Петра Великого.*
195251, Россия, г. Санкт-Петербург, Политехническая ул., 29
golubkovvd@gmail.com
ORCID: 0000-0001-9473-7430

СТРЕЛЕЦ Михаил Хаимович – *доктор физико-математических наук, заведующий лабораторией «Вычислительная гидроакустика и турбулентность» Высшей школы прикладной математики и вычислительной физики Санкт-Петербургского политехнического университета Петра Великого.*
195251, Россия, г. Санкт-Петербург, Политехническая ул., 29
strelets@mail.rcom.ru
ORCID: 0000-0002-4608-388X

Received 14.08.2024. Approved after reviewing 11.09.2024. Accepted 12.09.2024.
Статья поступила в редакцию 14.08.2024. Одобрена после рецензирования 11.09.2024. Принята 12.09.2024.